Recent Development of Volumetric PIV with a Plenoptic Camera

Brian S. Thurow[1] and Timothy Fahringer[1]

[1] Department of Aerospace Engineering, Auburn University, Auburn, AL, U.S.A.
thurow@auburn.edu

ABSTRACT

The recent development of a volumetric PIV system utilizing the unique light-field capturing capabilities of a plenoptic camera is described. The fundamental concept of a plenoptic camera, including a distinction between plenoptic 1.0 and plenoptic 2.0 is given, along with an illustration of the ability to computationally refocus an image after it has been acquired. A synthetic image generator for plenoptic cameras was developed and used to simulate plenoptic imaging of the motion of 3D particle fields. For volumetric reconstruction, the MART algorithm was adapted for use with the plenoptic camera through a reformulation of the weighting matrix that is consistent with the optical properties of the plenoptic camera. A prototype camera was designed and constructed based on the modification of a 16 MP PIV camera such that a microlens array can be mounted near the image sensor. This camera was used to show the proof-of-concept of the camera's ability to measure a 3D velocity field through experiments performed in a subsonic turbulent boundary layer and a supersonic jet. In both cases, the feasibility of plenoptic PIV was demonstrated with noted strengths being the simple set-up and operation of the system in addition to the ability to make 3D measurements over relatively large volumes.

1. Introduction

Since the advent of PIV, researchers have spent considerable time developing methodologies capable of measuring the flow velocity within a volume. These efforts have included stereographic [1], holographic [2-4], tomographic [5-7], laser sheet scanning [8-10] and defocusing PIV [11] among others. The complexity, accuracy and expense of each these techniques varies significantly with a full discussion of the strengths and weaknesses of each technique beyond the scope of this paper. In general, however, widespread adoption of these various 3D measurement techniques as standard PIV practice has been slow. In this work, we present recent progress in the development of a volumetric PIV technique utilizing the light-field capturing capabilities of a plenoptic camera. The primary advantage of 'plenoptic PIV' is that, being a single camera technique, it avoids the complexity and expense of a multi-camera system while retaining the ability to obtain 3D velocity measurements. As such, plenoptic PIV has the potential to be as robust, easy-to-use and economical as a traditional 2D PIV system. The paper begins with a brief description of light-field imaging and distinguishes between two types of plenoptic cameras that have recently become commercially available. The paper then continues with a description of our home-built plenoptic camera and briefly describes the tomographic methods that we employ for 3D image reconstruction. Lastly, we present some sample results highlighting the overall feasibility and capabilities of plenoptic PIV.

2. Light-Field Imaging and Plenoptic Camera

2.1 Fundamental Concept

The development of the plenoptic camera concept has evolved over the last couple decades beginning with the work of Adelson and Wang [12] and more recently refined by Ng. et al. [13] and Georgiev et al. [14, 15] for handheld photography and Levoy et al. [16] for microscopy. The latter works approach the problem from the perspective of light-field imaging, which describes the complete distribution of rays of light in space leading to a 5D function, sometimes termed the plenoptic function, where each light ray is characterized by its position (x, y, z) and angle of propagation (θ, φ). As light propagates through free space in a straight line, one of the dimensions is redundant and the resulting field is termed the 4D light-field. Standard photography only captures two dimensions of the 4D light-field as angular information is integrated, and therefore lost, at the sensor's surface. In contrast, a device that can record the complete 4D light-field would be of tremendous value. As described in Levoy [17], there are several ways to capture a light-field including the mounting of a camera on a gantry and taking a large number of photos at different positions, the use of a large array of cameras (as used in tomo-PIV [7] or synthetic aperture PIV [18]) or the use of a micro-lens array

mounted near a CCD to encode this information onto a single sensor. This last device, which is termed the plenoptic camera, records the light-field on a single image and is the central component of the work described herein.

Figure 1a illustrates the fundamental concept of the plenoptic camera. Similar to a conventional camera, a main imaging lens focuses light rays from the object plane to the image plane. Instead of an image sensor, however, a microlens array is positioned at the image plane. The function of each microlens is to focus the incident light onto the pixels behind the microlens where the incident angle of light striking the microlens determines which pixel will be illuminated. In this fashion, each microlens represents the position of a light ray at the image plane and each pixel represents the angle of propagation of that light ray. Taken collectively, the image recorded by the image sensor represents a sampling of the 4D light-field multiplexed onto a 2D image sensor.

a)   b)
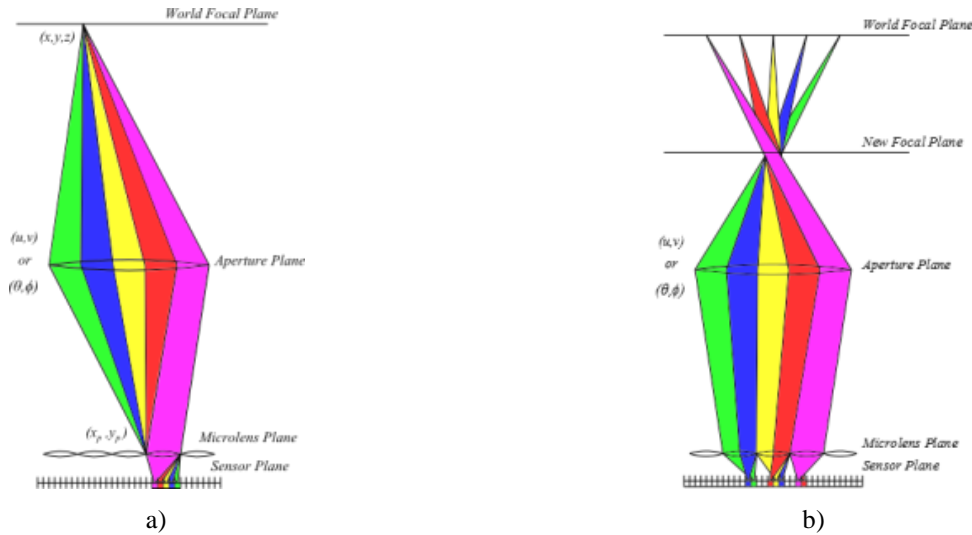
Figure 1 Schematic illustrating optical function of a plenoptic camera. A) A point source on the world focal plane is focused onto a single microlens illuminating all of the pixels underneath that microlens. B) By computationally combining information from different pixels, different light rays can be combined to yield new focal planes.

2.2 Computational Photography

Knowledge of a scene's light-field holds tremendous potential for a variety of applications. The most well-known use of light-field data is in the field of computational photography. In this field, light-field data is computationally processed to generate new images where the focus, depth-of-field and perspective can all be directly altered by the user. The ability to refocus an image *after it has been acquired* is the most noteworthy aspect of the consumer and machine vision plenoptic cameras developed by Lytro Inc. and Raytrix. Figure 1b illustrates the basic concept behind the refocusing procedure. As each pixel represents a different ray of light, one can choose different combinations of pixels (i.e. different light rays) and combine their information to render an image that appears as if a traditional camera was focused at a different depth. Figure 2 presents an example of this capability using an image acquired with our prototype camera (described later) and processed using an in-house refocusing algorithm.

a) near   b) mid   c) far
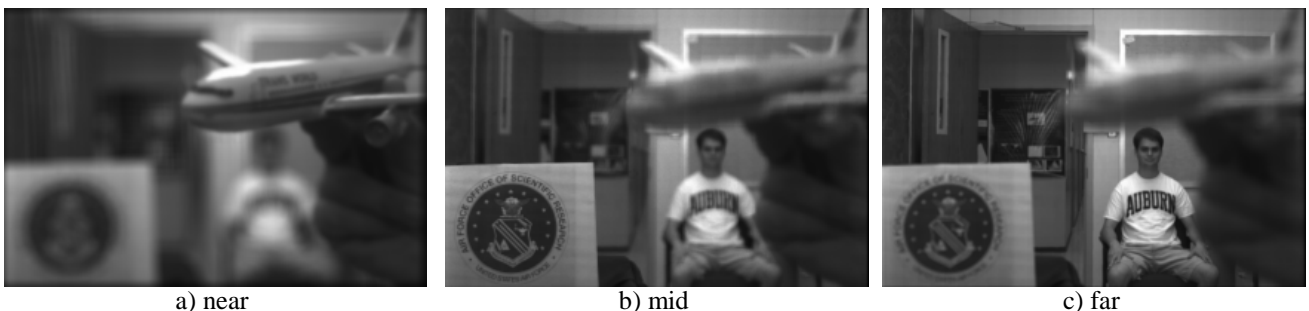
Figure 2 Example of ability to computationally refocus an image after it has been acquired with a plenoptic camera.

2.3 Plenoptic 1.0 vs Plenoptic 2.0

In the classical development of plenoptic cameras as detailed in Adelson and Wang [12] and Ng [13], the microlens array is placed one focal length away from the image sensor. In this fashion, each microlens is optically focused at 'infinity' such that the image formed by the microlens is simply an image of the main lens aperture. As the main lens

aperture is relatively far away compared to the focal length of the microlenses, the aperture appears to be 'in-focus' and each pixel behind the microlens simply corresponds to a different position on the main lens aperture. In this arrangement, it is straightfoward to represent the light-field using a *two-plane parameterization* where each light ray entering the camera is described by its point of intersection on the microlens array (physical x,y coordinate of the microlens) and point of intersection on the main lens aperture (u, v coordinate as given by the pixel coordinate relative to the microlens). Positioning the microlens array one focal length away from the image sensor is referred to as plenoptic 1.0 and is known to achieve the highest angular resolution for a given microlens. The main drawback of this approach, however, is a sacrifice in the spatial resolution of rendered images, which is nominally characterized by the number of microlenses contained in the array. The Lytro camera utilizes the plenoptic 1.0 concept for recording a light-field.

For conventional photography applications, it was soon realized that angular resolution could be sacrificed for additional spatial resolution while still retaining the ability to refocus or change the perspective of an image [14, 15]. This led to the development of plenoptic 2.0 cameras, also referred to as 'focused' plenoptic cameras, where the microlens array is positioned further than one focal distance away from the image sensor. As such, the image generated by each microlens is focused on a plane contained within the camera body (as opposed to the main lens). In this set-up, the main lens simply serves to map the 3D object space contained outside of the camera into a corresponding 3D image space in the camera's body. The function of each microlens then is to record a 2D image of the scene. In this sense, the microlens array can be interpreted as a large array (tens of thousands) of very low resolution (order 16 x 16 pixels) cameras recording an image of the scene from slightly different locations. High resolution images are then generated by stitching together the low-resolution images recorded by each microlens. As the images recorded by each microlens will overlap, some angular content is preserved such that refocusing and perspective views can still be generated. Depending on the degree to which the microlens images are focused, the plenoptic 2.0 concept allows for an adjustable tradeoff between spatial and angular resolution. Cameras commecially offered by Raytrix exploit this capability even further by utilizing arrays of microlenses with 3 different focal lengths such that the microlenses are optimized for different depths within the scene. For conventional photography, the plenoptic 2.0 concepts allows for a balance to be obtained between the resolution of rendered images and the ability to computationally change the focus and perspective of an image.

In this work, we utilize a plenoptic 1.0 camera. For our purposes, the plenoptic 1.0 concept provides an unambiguous measurement of the light-field such that adaptation and implementation of tomographic concepts (described shortly) for the reconstruction of volumes of particles is relatively straightforward. While the plenoptic 2.0 concept presents tangible benefits in conventional photography (mainly increased spatial resolution), the ambiguous relationship between spatial and angular resolution in these cameras makes it unclear how these benefits might apply to PIV. Many of the algorithms for rendering plenoptic 2.0 images implicitly assume that the scene consists of opaque objects located at a piecewise constant depth and without significant occlusions. In other words, the image formed by each microlens can be assigned a discrete depth value and stitched together with neighboring microlens images according to this assigned depth. In PIV, however, particles will be present throughout the entire volume such that each microlens can view multiple particle images simultaneously, with each particle possessing a different depth. As such, direct applications of these algorithms for PIV applications is not appropriate except under special conditions, such as low particle seed cocncentrations where only one particle will be seen at a time by a given microlens.

3. Prototype Camera

We have built our own prototype plenoptic camera by mounting a microlens array near the image sensor of a conventional PIV camera. The base camera is an Imperx Bobcat ICL-B4820, which incorporates a Kodak KAI-16000 interline CCD with 4872 x 3278 pixel resolution and 7.4 micron pixels. The microlens array consists of square microlenses with 125 micron pitch and 500 micron focal length such that approximately 288 x 194 microlenses cover the image sensor with approximately 16 x 16 pixels located underneath each microlens resulting in a 4D light-field resolution of approximately 288 x 194 x 16 x 16. A custom-designed mount is used to position the microlens array near the surface of the CCD and includes adjustment screws for the depth, tip and tilt of the array relative to the CCD. Alignment of the camera is achieved by removing the main lens and observing the focal spots produced by illuminating the exposed microlens array with a collimated light source. The position of the microlens array is manually adjusted until the focal spots are as small as possible and uniform across the array. The overall, one-time process takes about 10 - 15 minutes. An image of the fully assembled camera is shown in Figure 3. Most notable is the compact size of the camera and lack of moving parts. Operation of the camera is the same as that of a conventional camera.

Figure 3 Photograph of prototype plenoptic camera.

4. Synthetic Image Generation and Tomographic Reconstruction

To assist in the development of plenoptic PIV, a synthetic image generator was constructed to simulate the light-field data captured by a plenoptic camera. A brief description is provided here, however, more details can be found in [19]. The synthetic image generator uses simple ray transfer matrices to project light from a particle position through the optical path of the camera and to the CCD sensor. The microlens array is modeled using an extension of ray transfer matrices, referred to as 'affine optics' and detailed by [20]. 3D particle positions are specified in a frame of reference relative to the optical axis. A large number of rays of randomly varying angles are then projected (via ray transfer matrices) from the particle position to the image sensor to simulate the distribution of light rays scattered by an individual particle to the camera. For PIV, a large number of particles are generated with a random position and displaced to simulate a prescribed flow field (e.g. Oseen vortex, uniform flow, etc.). Comparison of sythetic image with real images indicate that this approach produces images consistent with those observed in experiments.

For reconstruction of particle volumes suitable for cross-correlation analysis, the MART algorithm used in tomo-PIV [7] was adapted for use with the plenoptic camera data. Our implementation is quite different, particularly with respect to the manner in which the weighting matrix is calculated. We use a series of light-field interpolations steps to estimate the relative amount of light that would be projected from each voxel in the reconstructed volume to each pixel in the captured plenoptic image. The process bears some similarity to the refocusing algorithm used to generate the images in Figure 2. The MART algorithm is then used with the weighting matrix to reconstruct an individual volume. For a full scale image, the weighting matrix is quite large (order 200 – 700 GB) and the process is computationally expensive and takes on the order of 10s of hours of processing time on a multi-core CPU depending on the size of the volume being reconstructed and the number of iterations. More details can be found in [21, 22]. Optimization of the algorithm for both accuracy and computational efficiency is ongoing.

Figure 4 shows a reconstruction of a small volume containing ~10,000 synthetically generated particles. Fig. 4a shows a 3D view of the particles where it can be observed that the reconstruction process results in elongated particles in the depth direction. This is due to the limited range of angles collected by the plenoptic camera, which is determined by the size of the main lens aperture and is currently a limiting factor of the technique. Figure 4b shows a projected view along the optical axis and illustrates that the lateral resolution of the particle positions is still quite accurate. As such, the depth resolution is seen to be poor compared to the lateral resolution. Work is currently ongoing to quantify this accuracy although preliminary results show better than 0.1 mm accuracy in lateral directions and better than 1.0 mm in depth for 1:1 imaging over a depth on the order of 50 mm. In addition, we have not seen any indication of ghost particles in the reconstructed volume which is believed to be due to the dense sampling of the angular space. For PIV, accurate displacement of the reconstructed particles is more important than the reconstruction quality. Displacements are caculated using a relatively conventional PIV cross-correlation algorithm adapted for 3D data. Figure 4c shows the 3D velocity field of an Oseen vortex as determined using plenoptic PIV and synthetic image data similar to that shown in Figs. 4a and 4b.
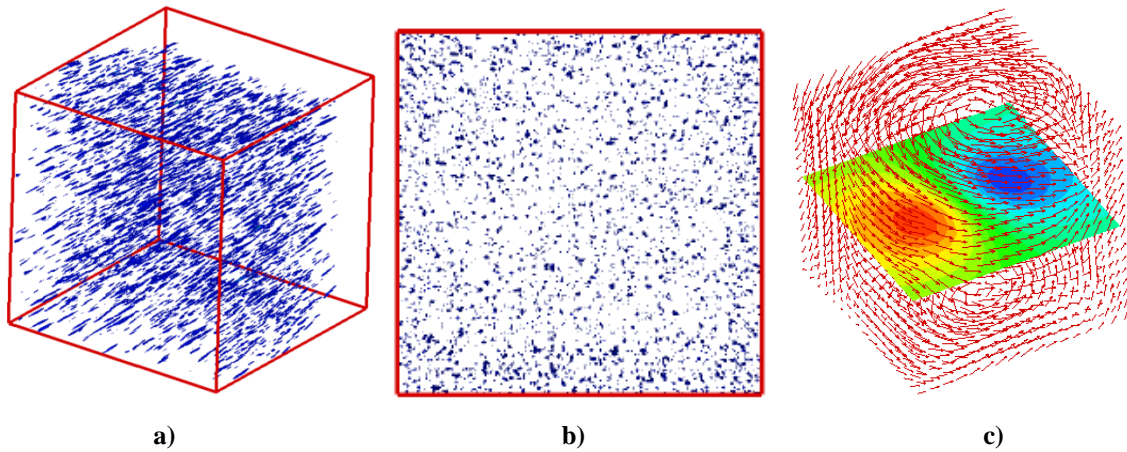
Figure 4 Volume reconstruction of a field of 10,000 synthetically generated particles. a) 3D view shows that reconstruction with MART algorithm results in elongated particles. b) Head on view shows resolution of MART in lateral directions. c) Example of 3D velocity field generated from synthetic data.

5. Experimental Results

To demonstrate the capability of the plenoptic camera to obtain 3D velocity measurements in a laboratory environment, we present two examples of recently obtained experimental results with our prototype camera. In both cases, the reults are preliminary as a full analysis of the flow field and comparison with traditional measurements is not included. Nonetheless, the results demonstrate the basic potential of the technique for 3D velocity measurements.

The first example is 3D measurement of an incompressible boundary layer with adverse pressure gradient. The boundary layer was formed on the test section wall of an open loop wind tunnel with free stream velocity of ~15 m/s. The plenoptic camera was positioned to image the boundary layer through a window looking up in the direction of shear (depth direction of the camera). The flow was seeded through an upstream slit with alumina particles and illuminated with a dual pulse laser outputting 50 mJ/pulse and formed into a 50 mm thick sheet. The Reynolds number based on momentum thickness, Re_θ, was 7,239 and the adverse pressure gradient (β=10.1) was imposed using a Stratford Ramp mounted on the opposite wall. Figure 5 shows the 3D velocity field determined using the plenoptic camera with dimensions highlighted in the figure. The streamwise velocity is indicated by the color of the vector; the shear of the boudnary layer is quite clear and the observed boundary layer thickness qualitatively agrees with that measured using traditional 2D PIV.
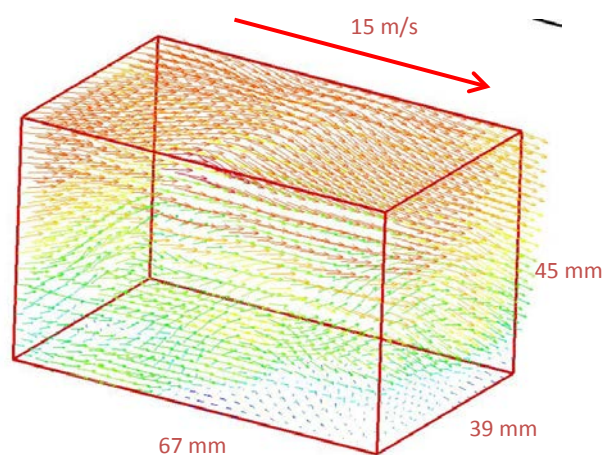
Figure 5 Preliminary experimental data showing 3D velocity field of a turbulent boundary measured using prototype plenoptic camera. Camera was oriented to look vertically up through the boundary layer illustrating ability to resolve shear along the optical axis.

The second example is taken from experiments recently conducted at the National Center for Physical Acoustics (NCPA) located at the University of Mississippi. These experiments were conducted as a proof-of-concept of the technique's viability for performing 3D velocity measurements in high Reynolds number, supersonic jet. The facility consists of a heated (T = 1005 K), 50.8 mm diameter, Mach 1.74 supersonic jet exhausting into an anechoic chamber. The jet nozzle is constructed from conic shaped converging and diverging sections that result in the production of shock-expansion cells even when the jet is operated at nominally ideally expanded conditions. The jet was seeded with submicron alumina particles injected through ports contained in the stagnation chamber. A volume of approximately 61 mm (streamwise) x 91 mm x 100 mm was illuminated using a pulsed Nd:YAG laser with pulse energy of approximately 200 mJ/pulse. Figure 6 shows a very preliminary result obtained from a single day of experiments. The color indicates the streamwise component of velocity with the y-axis (streamwise direction) stretched to show cross-sections of the jet at different downstream locations. The cross-sections spans approximately from x/D = 1.5 to 2.5. The ability of the camera to resolve the rough circular shape of the jet and the relatively thin shear layer is apparent although further work is needed to validate the small scale features observed around the jet periphery. LES performed in the same flow also indicates that variations in streamwise velocity within the jet core are to be expected in this flow.
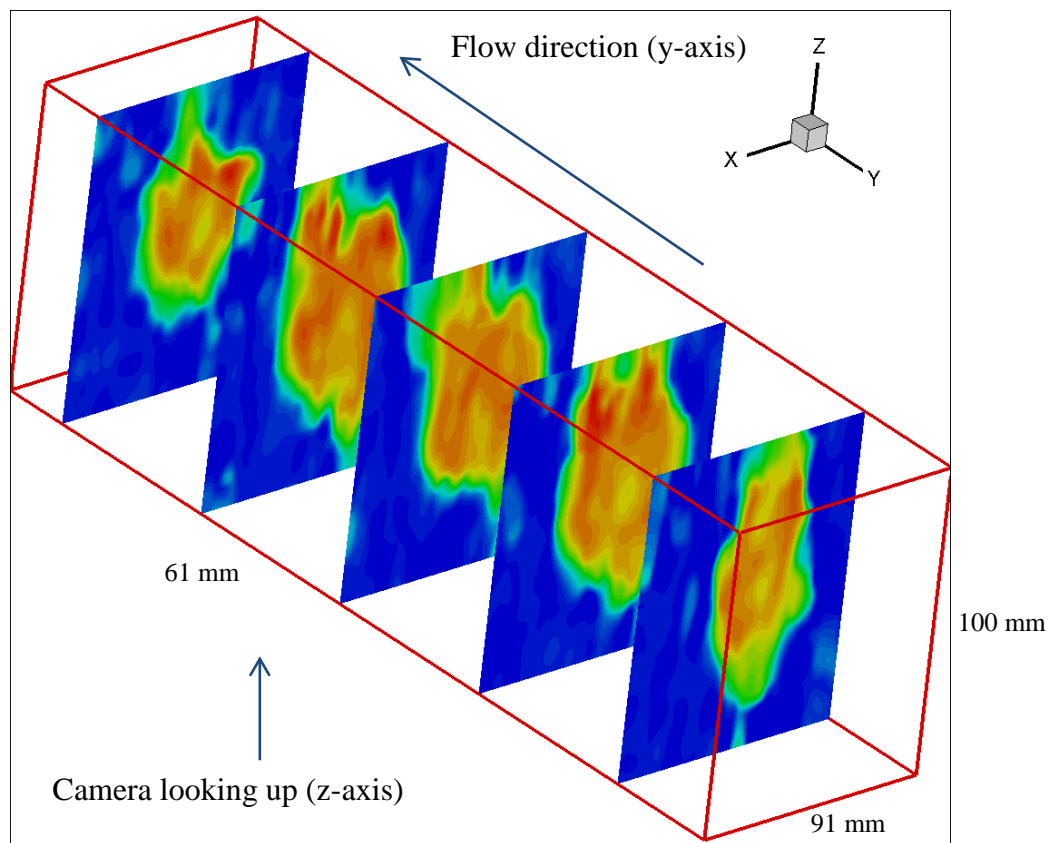
Figure 6 Sample 3D velocity field obtained in a 2" diameter supersonic jet seeded with alumina particles. Y-axis is stretch by factor of 5 to illustrate different cross-sections of jet flow. Color corresponds to streamwise (y) component of velocity.

6. Conclusions

Overall, plenoptic PIV appears to hold tremendous potential for simple and robust volumetric velocity measurements in a variety of flows. At this stage, the technique is still in its infancy and significant work is required to further characterize its strengths and weaknesses, particularly with respect to real-world issues such as variations in particle seed density, non-uniform illumination, etc. In addition, significant effort is needed and being placed on improving the computational efficiency of the volume reconstruction algorithms and increasing the accuracy and robustness of our 3D cross-correlation algorithm. Still, it is clear from these preliminary results that the primary advantage of plenoptic PIV is that it avoids the complexity and expense of a multi-camera tomo-PIV system while retaining the ability to obtain 3D velocity measurements. This is bolstered by the ability to make measurements over relatively thick volumes without the need for dramatic increases in laser energy. This is due to the fact that the technique works best when the main lens aperture is as wide open as possible, thus maximizing the amount of light collected by the camera. This is expected to improve even further in the future as we construct a new plenoptic camera based on a 29 MP CCD camera with a

sensitivity expected to be 5 times that of the prototype camera. Lastly, it is worth emphasizing that set-up and operation of the plenoptic PIV system is very similar to that of a traditional 2D PIV system. As such, plenoptic PIV has the potential to be as robust, easy-to-use and economical as a traditional 2D PIV system.

ACKNOWLEDGMENTS

REFERENCES

1. Guezennec, Y.G., et al., *Algorithms for fully automated three-dimensional particle tracking velocimetry.* Experiments in Fluids, 1994. **17**(4): p. 209-219.
2. Soria, J. and C. Atkinson, *Towards 3C-3D digital holographic fluid velocity vector field measurement—tomographic digital holographic PIV (Tomo-HPIV).* Measurement Science and Technology, 2008. **19**(7): p. 074002.
3. Trolinger, J.D., M. Rottenkolber, and F. Elandaloussi, *Development and application of holographic particle image velocimetry techniques for microgravity applications.* Measurement Science & Technology, 1997. **8**(12): p. 1573-1583.
4. Hinsch, K.D., *Holographic particle image velocimetry.* Measurement Science & Technology, 2002. **13**(7): p. R61-R72.
5. Scarano, F., *Tomographic PIV: principles and practice.* Measurement Science and Technology, 2013. **24**(1): p. 012001.
6. Elsinga, G.E., et al., *Tomographic 3D-PIV and applications.* Particle Image Velocimetry: New Developments and Recent Applications, 2008. **112**: p. 103-125.
7. Elsinga, G.E., et al., *Tomographic particle image velocimetry.* Experiments in Fluids, 2006. **41**(6): p. 933-947.
8. Hoyer, K., et al., *3D scanning particle tracking velocimetry.* Experiments in Fluids, 2005. **39**(5): p. 923-934.
9. Hori, T. and J. Sakakibara, *High-speed scanning stereoscopic PIV for 3D vorticity measurement in liquids.* Measurement Science & Technology, 2004. **15**(6): p. 1067-1078.
10. Brucker, C., D. Hess, and J. Kitzhofer, *Single-view volumetric PIV via high-resolution scanning, isotropic voxel restructuring and 3D least-squares matching (3D-LSM).* Measurement Science & Technology, 2013. **24**(2): p. 024001.
11. Pereira, F., et al., *Defocusing digital particle image velocimetry: a 3-component 3-dimensional DPIV measurement technique. Application to bubbly flows.* Experiments in Fluids, 2000. **29**(1): p. S078-S084.
12. Adelson, E.H. and J.Y.A. Wang, *Single lens stereo with a plenoptic camera.* Pattern Analysis and Machine Intelligence, IEEE Transactions on, 1992. **14**(2): p. 99-106.
13. Ng, R., et al., *Light Field Photography with a Hand-Held Plenoptic Camera*, 2005.
14. Georgiev, T. *New results on the Plenoptic 2.0 camera.* in *Signals, Systems and Computers, 2009 Conference Record of the Forty-Third Asilomar Conference on*. 2009.
15. Lumsdaine, A. and T. Georgiev. *The focused plenoptic camera.* in *Computational Photography (ICCP), 2009 IEEE International Conference on*. 2009.
16. Levoy, M., et al., *Light field microscopy.* ACM Trans. Graph., 2006. **25**(3): p. 924-934.
17. Levoy, M., *Light fields and computational imaging.* Computer, 2006. **39**(8): p. 46-+.
18. Belden, J., et al., *Three-dimensional synthetic aperture particle image velocimetry.* Measurement Science & Technology, 2010. **21**(12).
19. Lynch, K., *Development of a 3-D Fluid Velocimetry Technique based on Light Field Imaging*, in *Aerospace Engineering*2011, Auburn University.
20. Georgiev, T.I., C., *Light Field Camera Design for Integral View Photography*, A.S.T. Report, Editor 2006.
21. Fahringer, T. and B. Thurow. *Tomographic Reconstruction of a 3-D Flow Field Using a Plenoptic Camera.* in *42nd AIAA Fluid Dynamics Conference*. 2012. New Orleans, LA.
22. Fahringer, T. and B. Thurow, *The Effect of Grid Resolution on the Accuracy of Tomographic Reconstruction Using a Plenoptic Camera*, in *51st AIAA Aerospace Sciences Meeting including the New Horizons Forum and Aerospace Exposition*. 2013, American Institute of Aeronautics and Astronautics.